

On time dilation in quasar light curves

M. R. S. Hawkins¹^{*}

¹*Institute for Astronomy (IfA), University of Edinburgh, Royal Observatory, Blackford Hill, Edinburgh EH9 3HJ, UK*

Accepted 1988 December 15. Received 1988 December 14; in original form 1988 October 11

ABSTRACT

In this paper we set out to measure time dilation in quasar light curves. In order to detect the effects of time dilation, sets of light curves from two monitoring programmes are used to construct Fourier power spectra covering timescales from 50 days to 28 years. Data from high and low redshift samples are compared to look for the changes expected from time dilation. The main result of the paper is that quasar light curves do not show the effects of time dilation. Several explanations are discussed, including the possibility that time dilation effects are exactly offset by an increase in timescale of variation associated with black hole growth, or that the variations are caused by microlensing in which case time dilation would not be expected.

Key words: quasars: general – cosmology: observations.

1 INTRODUCTION

Time dilation (the stretching of time by a factor of $(1+z)$) is a fundamental property of an expanding universe. Given the success of the currently accepted cosmological model, which certainly implies expansion, it is perhaps surprising that more attention has not been paid to making direct measures of time dilation. This must surely be due in part to the fact that measures of time dilation can tell little or nothing about cosmological parameters within the framework of a Big Bang universe, but only whether or not the Universe is expanding. Also, it turns out to be surprisingly hard to formulate a conclusive test for time dilation. What is needed is an event or fluctuation of known rest frame duration which can be observed at sufficiently high redshift with an accuracy which enables the predicted stretching by a factor of $(1+z)$ to be observed.

The study of gamma-ray bursts has generated considerable interest in time dilation. The uncertainty in the intrinsic timescales of the bursts has made it difficult to measure time dilation directly, so earlier papers (for example (Deng & Schaefer 1998)) concentrated on demonstrating consistency when time dilation was allowed for. When redshifts of individual bursts became available more definitive tests were possible (Chang 2001), but correcting the raw data for selection effects involving an inverse correlation between luminosity and timescale has made the results hard to interpret with confidence. Rather than seeing gamma-ray bursts as providing a convincing test of time dilation, it is probably safer to say that if time dilation is a property of the Universe, then observations of gamma-ray bursts are consistent with this.

The light curves of distant supernovae provide a much more promising test for time dilation. Early work by (Goldhaber et al. 2001) which involved measuring the light curve widths of a sample of distant supernovae covering a wide range of redshifts, provided convincing evidence for the presence of cosmological time dilation. More recently, (Foley et al. 2005) have examined in detail the spectral evolution of a high redshift supernova, and shown that it is not consistent with no time dilation at a very high confidence level.

In this paper we address the question of whether time dilation is seen in quasar light curves. We use the light curves of over 800 quasars monitored on timescales from 50 days to 28 years to construct Fourier power spectra for high and low redshift samples, and compare their Spectral Energy Distributions (SEDs) to look for the effects of time dilation.

2 OBSERVATIONS

The observations upon which this paper is based come from two main sources. The first group are part of a long term monitoring programme undertaken by the UK Schmidt Telescope at Siding Springs Observatory in Australia from 1975 till 2002. The survey area comprises the central 20 square degrees of the ESO/SRC Field 287, centred on 21h 28m, -45° (1950). Some 300 plates were taken of this field in several passbands and over time intervals varying from an hour to 28 years. Part of the monitoring programme involved taking a sequence of plates in the B_J (IIIa-J/GG395) passband every year from 1975 to 2002, with the exception of 1976, and in most years at least 4 plates were obtained. In order to monitor time variability on shorter timescales, a second

* E-mail: mrsh@roe.ac.uk

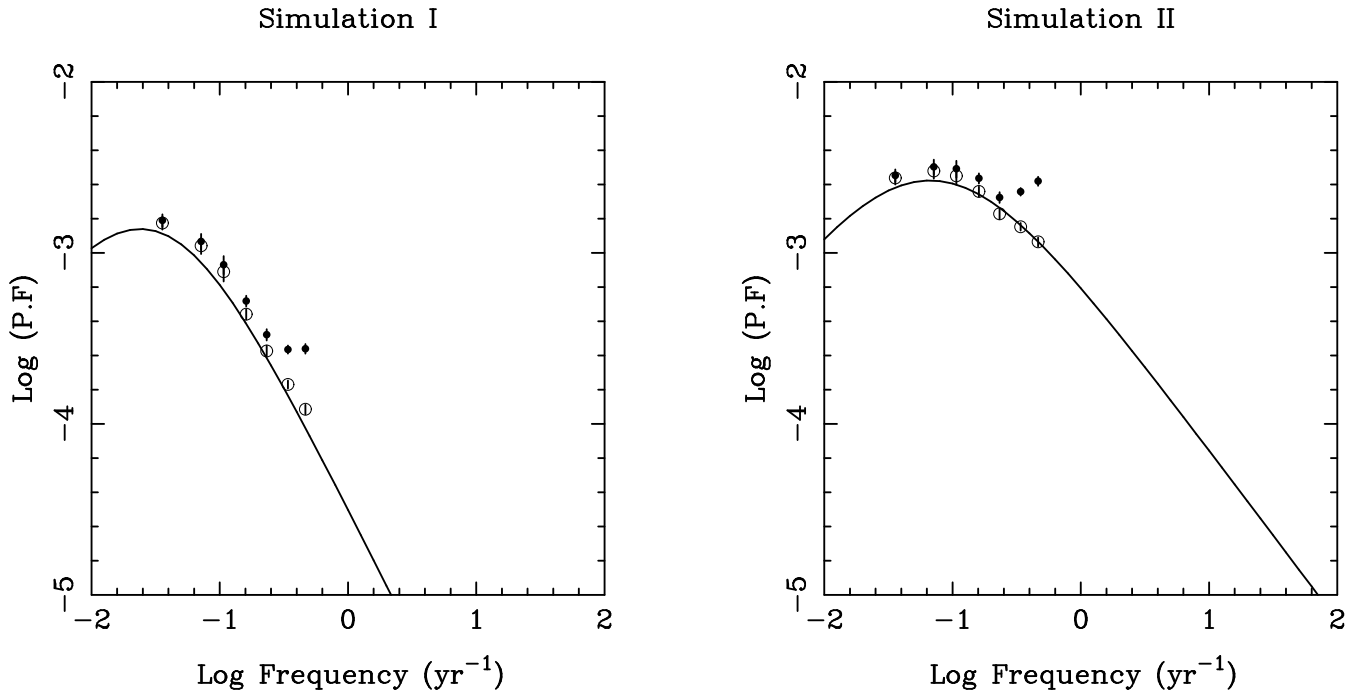


Figure 1. SEDs of sets of simulated light curves. The solid lines show the spectrum of variations used to construct the two different samples of light curves. Filled circles show the SEDs obtained by sampling as for the real data, and the open circles show the result of applying the sampling correction as described in the text.

sequence of 24 plates was taken from 1983 to 1985, covering the 2 year period as uniformly as possible.

The plates from the monitoring programme were measured by the SuperCOSMOS measuring machine at the Royal Observatory, Edinburgh to give catalogues of flux, position and image quality parameters. The raw magnitudes were calibrated with deep CCD sequences, and the results paired up to give a catalogue of some 200,000 objects to a completeness limit of $B_J = 21.5$, with magnitudes for the epoch corresponding to each plate. The plates were reduced to the same zero-point using local photometric transformations to minimise errors due to field effects across the plates, and light curves were constructed for every object in the catalogue from the mean magnitude for each year. The overall root mean square (rms) variation on the light curves due to photometric errors was estimated by measuring the rms variation of the light curves of samples of stars of similar colour and magnitude distribution to the quasars. The result, on the assumption that the stars were non-variable, was an rms of ± 0.05 mag.

Throughout the period in which Field 287 was being observed, intensive efforts were made to detect the quasars in the field. Given the nature of the survey material, quasars were most readily found from their variability. However, every other available technique was used to supplement this method, including ultra-violet excess, objective prism spectra, radio and X-ray surveys and two colour selection for high redshift objects. In the event most of the candidates which were identified as quasars after spectroscopic follow up were found by more than one technique, giving a good idea of the completeness of the final quasar catalogue. The

total number of quasars so far confirmed with redshifts now stands at over 1200 in the 20 square degrees of the survey area. Of these, 810 have no gaps in their light curves and make up a complete sample with well defined magnitude and position limits. This sample was used for the light curve analysis.

The second group of observations come from the monitoring programme of the MACHO project (Alcock et al. 1997). In this survey, which was primarily designed to detect microlensing events in the Magellanic Clouds and measure their light curves, an area containing several million stars was observed on average every few days over a period of about eight years. In addition, there has been a determined effort to detect any quasars lying in the survey area ((Geha et al. 2003), (Dobrzański et al. 2005) and references therein). Short timescale light curves for the 74 quasars with adequate photometry were constructed by binning the observations at 50 day intervals, giving a total of 49 epochs for each quasar. Of these, 68 lay within the luminosity bounds of the survey and were used in the light curve analysis.

3 LIGHT CURVE ANALYSIS

3.1 Fourier power spectra

The main purpose of this paper is to compare timescales of variation in low and high redshift samples of quasars. Fourier power spectrum analysis will be used to quantify the variation on different timescales, and to look for changes

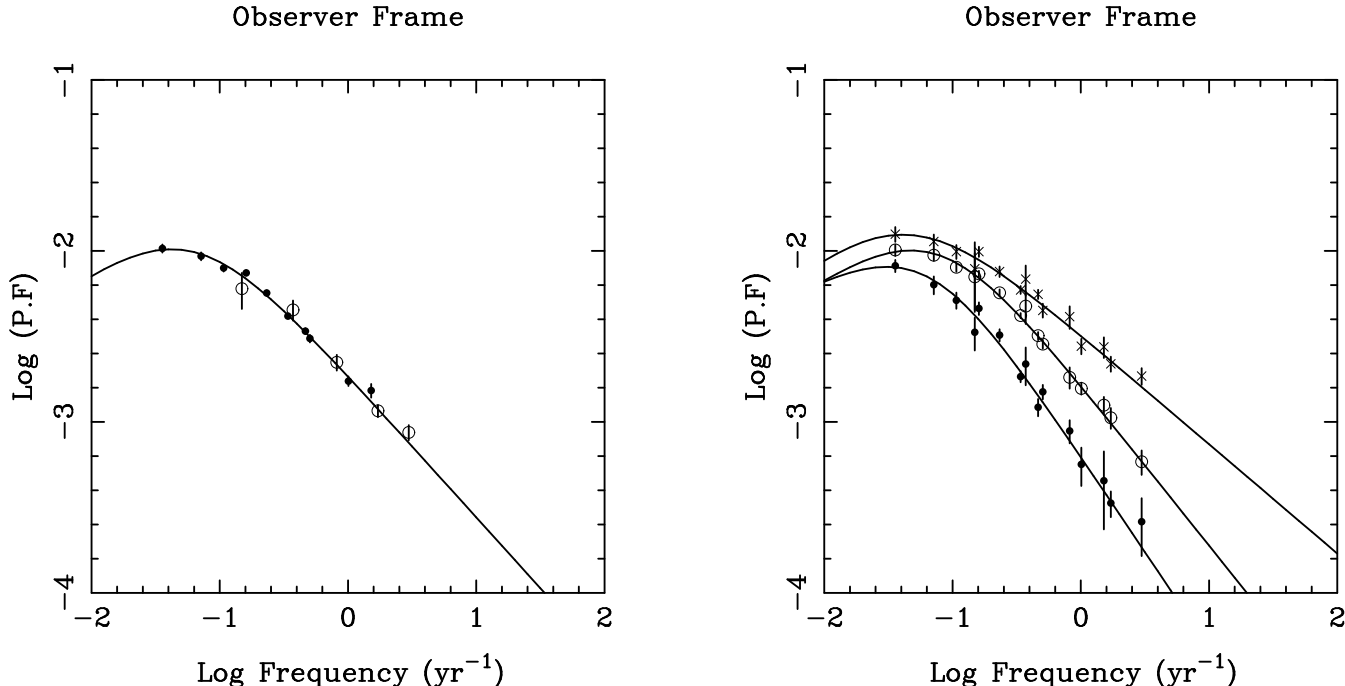


Figure 2. The left hand panel shows SEDs of light curves in the observer frame for quasars from the Field 287 survey (filled circles) and from the MACHO project (open circles). The solid line is the best fit of the curve in Eq. 2. The right hand panel shows the same data divided into three magnitude ranges as defined in Table 1. In this case filled circles, open circles and stars represent high, medium and low luminosity bins respectively. Solid lines are fits to the data as for the left hand panel.

with redshift. We define the Fourier power spectrum $P(s)$ as:

$$P(s_i) = \frac{\tau}{N} \left(\sum_{j=1,N} m(t_j) \cos \frac{2\pi i j}{N} \right)^2 + \frac{\tau}{N} \left(\sum_{j=1,N} m(t_j) \sin \frac{2\pi i j}{N} \right)^2 \quad (1)$$

where i runs over the N equally spaced epochs of observation separated by time τ , and $m(t_j)$ is the magnitude at epoch t_j . In the case of a sample of light curves, the integration for each frequency continues over all sample members.

Since quasars typically vary on timescales of as little as a few months, the power spectra of the light curves with several observations averaged to give measures for yearly epochs must be corrected for the actual sampling pattern. This was done by constructing simulated light curves with fully sampled epochs of observation, and with sampling identical to the times of the actual observations, with a resolution of 0.1 years. The simulations were carried out along the lines advocated by (Timmer & König 1995). Fourier power spectra were then calculated for sets of 1000 simulated light curves with full and actual sampling, and the correction obtained as the difference between the two. This correction was then applied to the power spectrum of each of the observed light curves. The effect of the sampling correction is illustrated in Fig. 1, which shows SEDs for simulated light curves with widely different modes of variation. (For the purposes

of this paper, we define the SED as a plot of the product of Fourier power and frequency versus frequency.) The solid line shows the spectrum of variations on which the simulations were based. Also shown are the SEDs of the simulated light curves sampled as for the actual data, and the effect of applying the sampling correction.

A second correction was also necessary to allow for the effects of Poisson noise in the observed light curves as discussed by (Hawkins 2007). The Poisson noise level was measured by calculating the Fourier power spectra for large samples of stars, assumed to be non-variable. This correction, which was quite small, was subtracted from the integrated power spectra of the samples of light curves. Fourier power spectra of the three sets of light curves defined in Section 2 were calculated as described above, and are plotted as SEDs in the left hand panel of Fig. 2. It will be seen that all three SEDs are in good agreement in the areas of overlap, giving confidence that there were no residual systematic effects in the data.

In order to obtain a measure of timescale and other parameters, the SEDs were fitted by the function:

$$P(f) = \frac{C}{\left(\frac{f}{f_c}\right)^a + \left(\frac{f}{f_c}\right)^{-b}} \quad (2)$$

This function has the form of a power law rise from short timescales, turning over at a characteristic timescale $\tau = f_c^{-1}$. The maximum power density occurs at timescale t_{max} given by:

$$t_{max} = \tau \left(\frac{a}{b} \right)^{\frac{1}{a-b}} \quad (3)$$

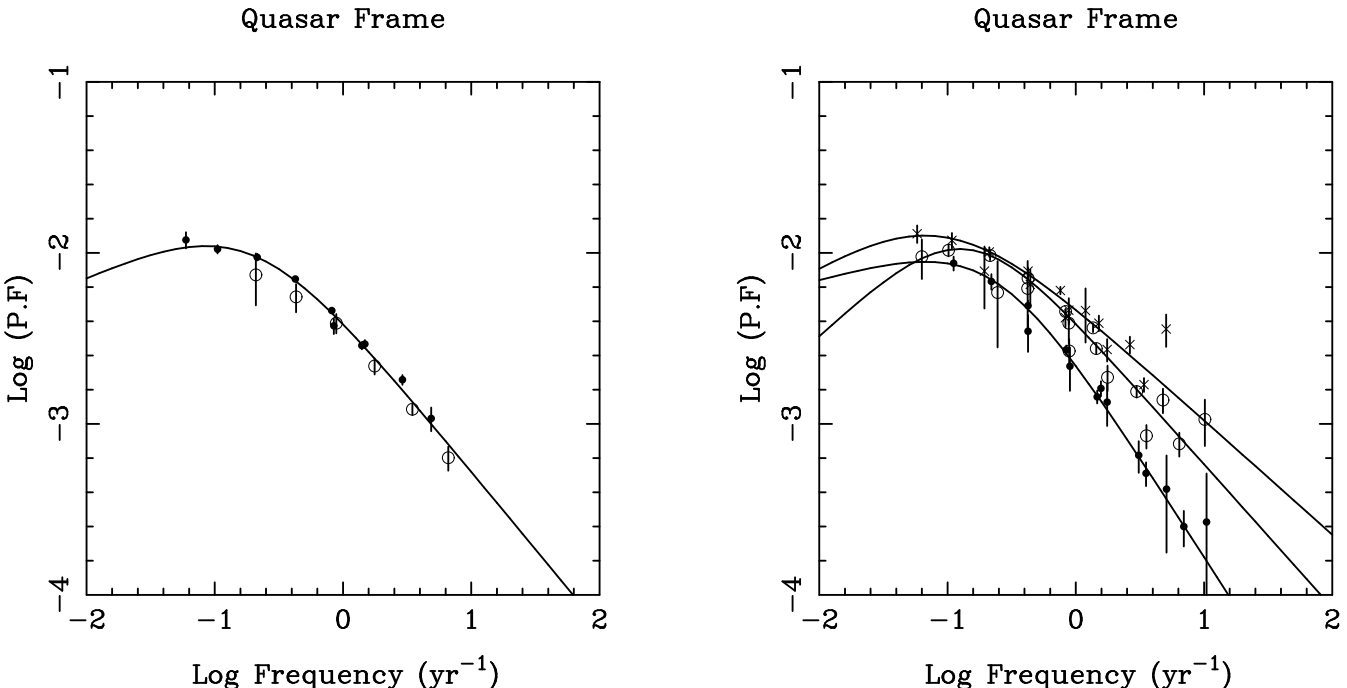


Figure 3. Same as for Fig. 2 but with a correction for time dilation applied to the SEDs.

The function $P(f)$ was fitted iteratively to the data in the left hand panel of Fig. 2, and the best fit is shown as a solid line. Best fit values for the parameters t_{max} and τ are given in Table 1 together with the sample size, the asymptotic value of the slope or power law index towards short timescales ($-a$), and the χ^2 value of the fit. With 14 degrees of freedom, the fit is clearly satisfactory.

The errors on the model parameters were estimated by repetitively selecting half the sample at random, and carrying out the fitting procedure. The errors were then calculated from the measured dispersion in the parameter values and are shown in Table 1.

Preliminary examination of the left hand panel of Fig. 2 suggests that the data follow a power law rise from high frequency (short timescale) variation which breaks at a timescale of about 5 years to reach a maximum power density at around 25 years. The position of this maximum is however not well defined due to lack of long timescale measurements.

3.2 Magnitude effects

The idea that there is a correlation between the way quasars vary and their absolute magnitude or luminosity has a long history. In particular, several authors (Hook et al. 1994; Cristiani et al. 1996; Hawkins 2000) have claimed to find an anti-correlation between luminosity and amplitude, in the sense that for a sample of quasar light curves, more luminous quasars are seen to vary over a smaller range of brightness than less luminous ones. One of the problems with this conclusion is that the observed amplitude is clearly a function of the length of the run of observations, and so can be confused with timescale of variability. Fourier analysis pro-

vides a way round this by giving measures of variability on different timescales. In the right hand panel of Fig. 2 the data in the left hand panel is divided into three luminosity ranges and the SEDs fitted with the function $P(f)$ in Eq. 2 as for the left hand panel.

The three curves in the right hand panel of Fig. 2 show broadly the same features as the curve in the left hand panel, but it is clear that the anti-correlation between luminosity and amplitude is confirmed. The maximum power density of the lowest luminosity quasars is greater than the highest by a factor of 1.5. In this case it appears that the time span of the data is sufficient to resolve the degeneracy between timescale and amplitude.

A striking feature of the three SEDs is the difference in the power law indices at high frequencies. It appears that there is a very marked decrease in the amount of short timescale variation as quasars become more luminous. The analysis of this intriguing result is beyond the scope of the present paper, but we note it here because of its possible effect on the measurement of time dilation, and will discuss it further in Section 4.

Of great interest is the timescale at which the three SEDs reach their maximum power density. Unfortunately, lack of longer timescale data makes the exact positions uncertain, and it would be premature to identify any trend of this parameter with luminosity. In fact, all three measures of t_{max} in Table 1 are consistent within the errors with having the same value.

Table 1. Timescale parameters for magnitude and redshift limited samples of quasar light curves in the observer and quasar frames.

sample	mean	size	τ (years)	t_{max} (years)	index	t_{ref} (years)	χ^2
observer frame							
all quasars		878	17.0 ± 1.6	23.2 ± 0.9	-0.83 ± 0.02	2.4	14.8
$-23.5 < M_B$	$< M_B > = -22.64$	217	23.2 ± 1.6	23.5 ± 2.1	-0.64 ± 0.02	1.3	11.1
$-25.5 < M_B < -23.5$	$< M_B > = -24.55$	484	13.3 ± 0.9	20.6 ± 1.1	-0.94 ± 0.02	2.5	6.1
$M_B < -25.5$	$< M_B > = -26.09$	177	15.6 ± 1.4	31.4 ± 6.2	-1.12 ± 0.05	5.0	12.9
$z < 1.0$	$< z > = 0.765$	171	16.3 ± 1.9	27.7 ± 5.0	-0.81 ± 0.05	2.2	9.6
$z > 1.0$	$< z > = 1.711$	469	14.2 ± 1.0	20.3 ± 1.0	-0.88 ± 0.02	2.2	7.3
quasar frame							
all quasars		878	5.2 ± 0.4	11.5 ± 0.6	-0.91 ± 0.03	0.9	16.5
$-23.5 < M_B$	$< M_B > = -22.64$	217	10.7 ± 4.2	14.3 ± 7.6	-0.67 ± 0.05	0.7	30.6
$-25.5 < M_B < -23.5$	$< M_B > = -24.55$	484	7.0 ± 0.4	7.8 ± 0.8	-0.84 ± 0.02	1.0	37.4
$M_B < -25.5$	$< M_B > = -26.09$	177	4.1 ± 0.3	14.4 ± 3.4	-1.17 ± 0.04	1.5	5.1
$z < 1.0$	$< z > = 0.765$	171	7.4 ± 0.6	15.2 ± 2.9	-0.87 ± 0.05	1.2	14.9
$z > 1.0$	$< z > = 1.711$	469	6.8 ± 0.6	7.4 ± 0.4	-0.82 ± 0.03	0.8	5.2

4 TIME DILATION

4.1 The quasar frame

The SEDs in Fig. 2 represent timescales in the observer's reference frame, and describe variations as measured from Earth. If it is assumed that these variations in flux are intrinsic to the quasars, then the timescales will be subject to the effects of time dilation. If we wish to recover the timescales as they would be seen in the rest frame of the quasar, it is necessary to change the unit of time for each individual light curve for a quasar of redshift z by a factor $(1+z)^{-1}$, and hence the frequency scale by a factor $(1+z)$. This leads to a modification of Eq. 1 such that

$$\tau \rightarrow \frac{\tau}{1+z} \quad (4)$$

As well as re-scaling by a factor of $(1+z)$ along the time axis, there is an additional correction to make to the normalisation by a factor of $(1+z)$, to keep the power the same in the observed and time-shifted light curves.

Fig. 3 shows the effect of applying the correction for time dilation to the data in Fig. 2. The SEDs are fitted with the function $P(f)$ defined in Eq. 2 as before, and the best-fit parameters are given in Table 1. Broadly speaking, the effect of correcting for time dilation is to shift each of the curves to shorter timescales by a factor $(1+<z>)$, where $<z>$ is the mean redshift of the objects in the magnitude bins. There is a marked increase in the scatter

in the data after they have been corrected for time dilation, but the maximum power density is not changed. In order to quantify any shift in timescale after correcting for time dilation, we define a reference time t_{ref} as the timescale at which $\log(P(f)) = -2.4$. Values of t_{ref} are also given in Table 1.

4.2 Measurements of time dilation

One of the difficulties in looking for correlations in the properties of quasars is the well known degeneracy between redshift and luminosity in magnitude limited samples. The degeneracy takes the form of a correlation between redshift and luminosity such that in most available samples the higher redshift members tend to be the more luminous. Thus if we are looking for a correlation between redshift and timescale, as in time dilation, we must be careful that we do not actually measure a correlation between luminosity and timescale. We have shown in Section 3 above that for the samples of quasars under consideration here, we find an anti-correlation between quasar luminosity and Fourier power density. This in itself would not necessarily be a problem, but the SEDs also show a correlation between luminosity and the rate at which short timescale power density declines. Given the correlation between redshift and luminosity, such an effect could be confusing in a search for a correlation between redshift and timescale as expected for time dilation. To minimise

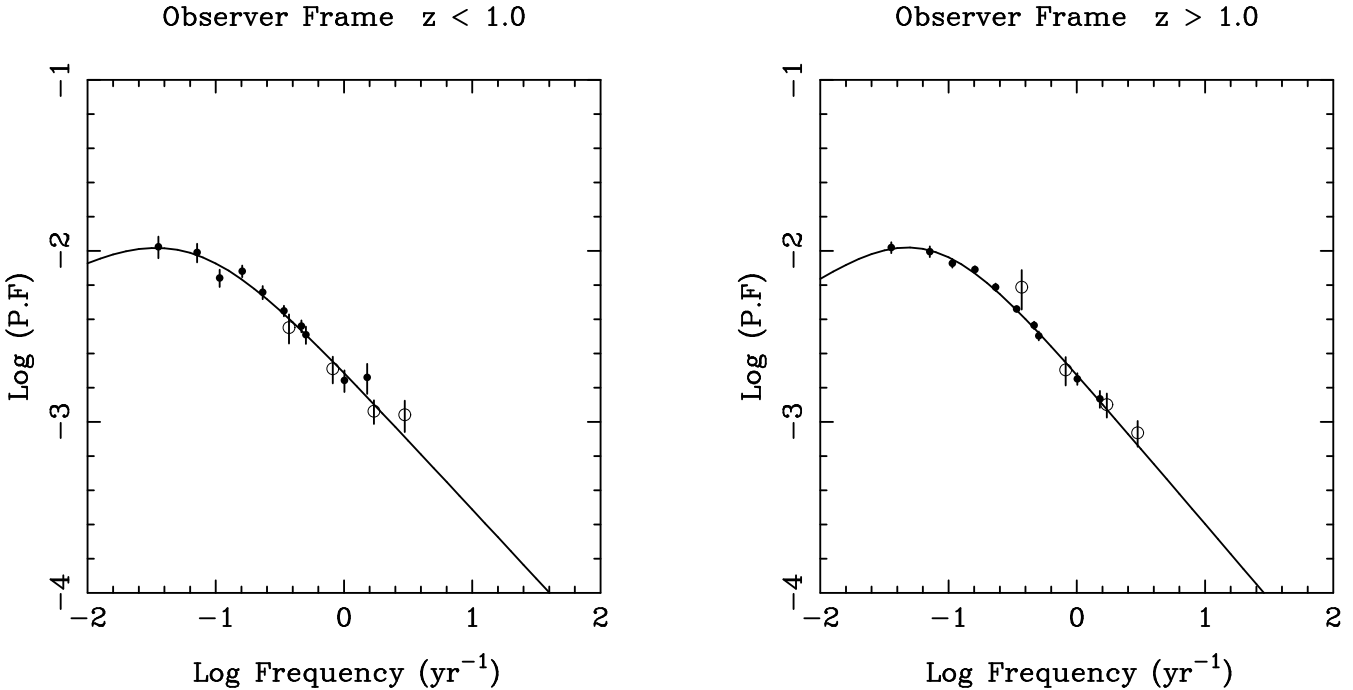


Figure 4. The left and right hand panel show SEDs of light curves in the observer frame for low and high redshift samples of quasars respectively. The symbols and solid line are as for the left hand panel of Fig. 2.

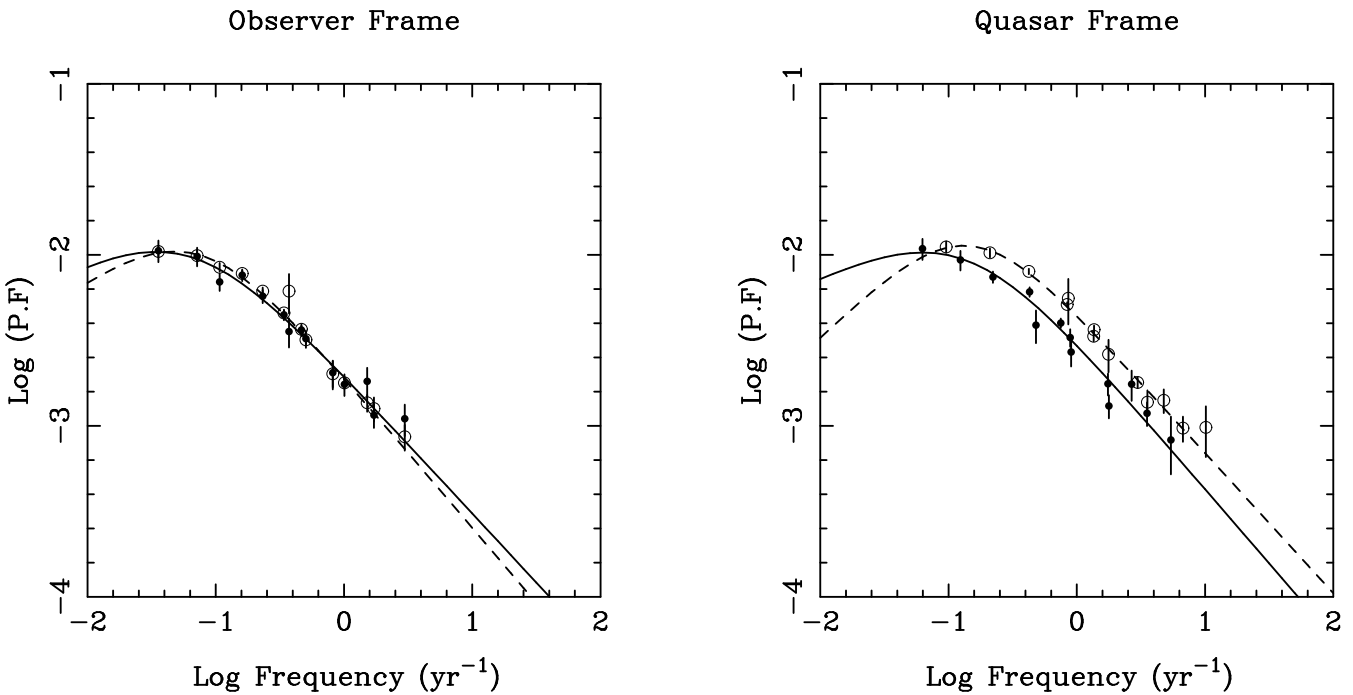


Figure 5. The left hand panel shows the superposition of the SEDs for low and high redshift samples of light curves from Fig. 2. The right hand panel shows SEDs of the same light curves in the quasar frame, with a correction for time dilation applied.

any such effect the absolute magnitude range of quasars was restricted to the band $-25.5 < M_B < -22.5$, which is sufficiently small that no correlation of amplitude with luminosity is detectable. This also has the effect of reducing any contamination from host galaxy light to a negligible level.

In order to measure the effects of time dilation we split the quasar light curves into low and high redshift samples. The idea was to compare the resulting SEDs to look for the expected shift of the high redshift sample towards longer timescales relative to the low redshift sample. Fig. 4 shows the low and high redshift SEDs separately, and it can be seen that in spite of the restriction in luminosity the SEDs are well defined, with excellent agreement between the different datasets where they overlap. The data are well fitted by the function $P(f)$ in Eq. 2, and the fit parameters of interest are given in Table 1.

Fig. 5 shows the effect of correcting the SEDs in Fig. 4 for time dilation. The left hand panel shows the two SEDs in the observer frame superimposed to show any shift in timescale. The right hand panel shows the same data with the correction for time dilation applied. It is immediately clear that in the observer frame the two SEDs are very closely matched, with $t_{ref} = 2.2$ years in both cases. However, in the quasar frame there is a marked difference, the high redshift quasars being preferentially shifted to shorter timescales. It will be noticed that the maximum power density of both high and low redshift SEDs is the same in the quasar and observer frames, implying that the shift in the position of the SEDs is in timescale. The ratio of the values of t_{ref} for the high and low redshift samples is almost exactly equal to the ratio of the values for $(1 + \langle z \rangle)$, implying that the effect of correcting for time dilation has been to move the SEDs to shorter timescales by a factor of $(1 + \langle z \rangle)$, with no other obvious change.

5 INTERPRETATION OF RESULTS

The results of Section 4 provide strong evidence that the effects of time dilation are not seen in quasar light curves. This clearly runs against expectations based on a conventional cosmological viewpoint, and so in this section we examine ways in which the results may be understood.

5.1 Black hole growth

Perhaps the most straightforward way of explaining the absence of the effects of time dilation in quasar light curves is to postulate an increase in timescale of variation associated with the growth of the central supermassive black hole of the AGN. Thus higher redshift quasars would contain less massive black holes which would vary more quickly in such a way as to offset the effects of time dilation. The problem with this picture is that there is a well-supported correlation between black hole mass and luminosity based on reverberation mapping (Kaspi et al. 2000). This means that, given the restricted magnitude range of our sample, there can be little difference in the average black hole mass of the high and low redshift samples. Even if we ignore the restriction on luminosity, it would be difficult to cancel out time dilation effects by assuming an increasing luminosity with redshift

as it is clear from Fig. 3 that the whole shape of the SED changes with luminosity, especially the power law index to shorter timescales. This is not what is seen in Fig. 5, where the shape of the SEDs does not change between high and low redshift samples.

5.2 Microlensing

Another possibility for explaining the absence of time dilation effects in quasar light curves is that the variations do not predominantly originate in the quasars, but along the line of sight at low redshift. The most plausible mechanism for this is microlensing of the quasars by a population of stellar mass bodies (Hawkins 2007), where the most probable redshift for the lenses is $z \sim 0.5$ (Turner et al. 1984). Although such microlensing is unambiguously seen in multiple images of gravitationally lensed systems (Pelt et al. 1998), there are two main difficulties with this approach. Firstly, although the observed variations agree well with model predictions from microlensing simulations, it is difficult to rule out the possibility of intrinsic variations. Secondly, it appears that the rate of detection of compact bodies in the Galactic halo by the MACHO project (Alcock et al. 1997) is incompatible with the population required to produce the observed variation in the quasar light curves.

5.3 Static universe

The well known dilemma that Einstein was faced with when he realised that his equations implied an expanding universe is still perhaps the best reason for believing that the universe is not static, given the success of general relativity in explaining cosmological observations. There is however surprisingly little direct evidence that the Universe is expanding. As mentioned in Section 1, searches for time dilation in gamma-ray bursts do not provide a conclusive test. Supernova light curves on the other hand appear to show convincing evidence of time dilation (Foley et al. 2005), which would rule out a non-expanding universe as an explanation for the results presented here for quasar light curves. Although this result has been challenged in an interesting paper by (Crawford 2009) on the basis of bias in the sampling procedure, it seems fair to say that the result is still generally accepted.

5.4 Quasar distances

For completeness we should add that a possible explanation for the apparent lack of time dilation effects in quasar light curves is that quasars are not at the cosmological distances implied by their redshifts. This idea has been energetically pursued by examining apparent associations of quasars with relatively nearby galaxies or clusters (Arp & Russell 2001), but the large body of observations of quasar host galaxies seems to rule out the possibility that quasars are nearby, and that as a result time dilation would be negligible.

6 DISCUSSION

Taken at face value, the observations described above can only be explained by at least a small departure from the

conventional cosmological view, and perhaps a large one. It is therefore worth reviewing the security of the observational results to be sure that they are robust. We need to check that the data are showing a consistent picture. We first note that the Field 287 and MACHO data are completely independent of each other in that they contain different sets of quasars selected according to different criteria in different areas of sky. The photometric monitoring was carried out using completely different techniques with different error distributions, and yet for all the SEDs presented above, in the area of overlap the agreement between the two datasets is excellent. The implication of this is that the shape of the SEDs represents a true signal, and is not dominated by systematic effects.

In the right hand panel of Fig. 2 the only difference between the three SEDs is the quasar luminosity, and yet a clear progression in slope of the power law index at short timescales is evident, implying a real and measurable change in the nature of the variability, and not an artefact of the analysis procedure. This provides sound support for believing that the close similarity of the high and low redshift SEDs in Fig. 5 represents indistinguishable patterns of variability, unaffected by any time dilation effect, and not a spurious agreement.

If it is accepted that time dilation is not seen in quasar light curves, then some departure from conventional cosmology is necessary to explain it. Of the possibilities listed in Section 5, there seems to be overwhelming evidence that quasars are at the cosmological distances indicated by their redshifts, and the challenge to the time dilation found in supernovae light curves has yet to be convincingly established. If we therefore assume that we live in an expanding universe, we have two possibilities. If the variations are due to microlensing then the conclusions of the MACHO project would have to be modified, presumably by a reassessment of the shape of the Galactic halo, and the expected dark matter content. If the effects of time dilation are offset by an increase of timescale of variation with cosmological time, then a mechanism must be found which does not alter the shape of the SED, or involve a correlation of black hole mass with luminosity.

7 CONCLUSIONS

In this paper we have used Fourier power spectrum analysis of over 800 quasar light curves to measure timescales of variation at different redshifts. The expected effects of time dilation are absent, the SEDs at high and low redshift being essentially identical. There seems to be no explanation for this within the conventional cosmological framework, and so various other possibilities are considered. These include the idea that the effects of time dilation are exactly offset by an increase in timescale of variation associated with black hole growth. Alternatively, the observed variations could be caused by microlensing, in which case time dilation would not be expected.

ACKNOWLEDGEMENTS

I thank Alan Heavens for suggesting the procedure for verifying the effectiveness of the sampling correction.

REFERENCES

- Alcock C. et al., 1997, ApJ, 486, 697
- Alcock C. et al., 2001, ApJ, 550, L169
- Arp H., & Russell, D. 2001, ApJ, 549, 802
- Chang, H.-Y. 2001, ApJ, 557, L85
- Crawford, D.F. 2009, arXiv:0901.4172
- Cristiani, S., Trentini, S., La Franca, F., Aretxaga, I., Andreani, P., Vio, R., Gemmo, A. 1996, A&A, 306, 395
- Deng, M., & Schaefer, B.E. 1998, ApJ, 502, L109
- Dobrzański, A., Eyer, L., Stanek, K.Z., Macri, L.M. 2005, A&A, 442, 495
- Foley, R.J. et al. 2005, ApJ, 626, L11
- Geha, M. et al. 2003, AJ, 125, 1
- Goldhaber, G. et al. 2001, ApJ, 558, 359
- Hawkins, M.R.S. 2000, A&AS, 143, 465
- Hawkins, M.R.S. 2007, A&A, 462, 581
- Hook, I.M., McMahon, R.G., Boyle, B.J., Irwin, M.J. 1994, MNRAS, 268, 305
- Kaspi, S., Smith, P.S., Netzer, H., Maoz, D., Jannuzi, B.T., Giveon, U. 2000, ApJ, 533, 631
- Pelt, J., Schild, R., Refsdal, S., Stabell, R. 1998, A&A, 336, 829
- Timmer, J., & König, M. 1995, A&A, 300, 707
- Turner, E.L., Ostriker, J.P., Gott, J.R. 1984, ApJ, 284, 1